Available online at www.sciencedirect.com
ScienceDirect
Microporous and Mesoporous Materials 102 (2007) 178–187
MICROPOROUS AND MESOPOROUS MATERIALS
www.elsevier.com/locate/micromeso

Partially graphitic, high-surface-area mesoporous carbons from polyacrylonitrile templated by ordered and disordered mesoporous silicas

Michal Kruk [a,*,1], Kevin M. Kohlhaas [b], Bruno Dufour [a,2], Ewa B. Celer [c], Mietek Jaroniec [c], Krzysztof Matyjaszewski [a,*], Rodney S. Ruoff [b], Tomasz Kowalewski [a,*]

[a] *Department of Chemistry, Carnegie Mellon University, 4400 Fifth Avenue, Pittsburgh, PA 15213, USA*
[b] *Department of Mechanical Engineering, Northwestern University, Evanston, IL 60208, USA*
[c] *Department of Chemistry, Kent State University, Kent, OH 44242, USA*

Received 23 September 2006; received in revised form 12 December 2006; accepted 14 December 2006
Available online 21 December 2006

Abstract

Ordered and disordered mesoporous carbons synthesized from polyacrylonitrile using a templating method were heated under argon atmosphere at ~2470 K to partially graphitize them without the loss of mesoporosity. The high-temperature treatment led to a marked enhancement of graphitic ordering, which manifested itself in a narrowing of wide-angle XRD peaks, and in the appearance of domains of lateral dimensions 5–15 nm, consisting of stacked graphitic planes with interplanar spacing of ~0.34 nm. Raman spectroscopy provided evidence for the increased content of graphitic sp^2 carbon structures. The specific surface areas and total pore volumes of the carbons were as high as 500–600 $m^2\ g^{-1}$ and 0.8–1.8 $cm^3\ g^{-1}$, respectively. These carbons had essentially no microporosity and their surface properties were similar to those of a graphitized carbon black Carbopack X. For ordered mesoporous carbons, the high-temperature treatment led to the loss of nanoscale periodicity, broadening of the pore size distribution (PSD) and ~40% decrease in the mesopore volume. In contrast, PSD and total pore volume of the disordered carbon were essentially unchanged. These results show that the high-temperature treatment of mesoporous carbons from PAN affords partially graphitic carbons with high specific surface areas and large pore volumes.

Keywords: Mesoporous carbon; Graphitization; Templated synthesis; High-surface-area solid; Polyacrylonitrile

1. Introduction

Graphitic mesoporous carbons (that is, those with pores of diameter 2–50 nm) are attractive materials for many applications, including liquid chromatography [1–3], adsorption, and manufacturing of electrochemical double-layer capacitors and Li-ion batteries. Graphitic carbons exhibit enhanced thermal stability and electrical conductivity, and have unique adsorption properties related to their highly homogeneous surfaces [1–3], in addition to their high degree of chemical inertness. Carbon structures with an appreciable degree of ordering of graphene sheets typically form as a result of a heat treatment at 2300–3300 K under inert atmosphere (argon, nitrogen) [4]. This high-temperature treatment is often referred to as "graphitization", although its outcome depends not only on temperature (and other conditions), but also on the properties of the carbon sample subjected to heating. The addition of

* Corresponding authors. Tel.: +1 718 982 4030; fax: +1 718 982 3910.
E-mail addresses: kruk@mail.csi.cuny.edu (M. Kruk), r-ruoff@northwestern.edu (R.S. Ruoff), jaroniec@kent.edu (M. Jaroniec), km3b@andrew.cmu.edu (K. Matyjaszewski), tomek@andrew.cmu.edu (T. Kowalewski).
[1] Present address: Department of Chemistry, College of Staten Island and Graduate Center, City University of New York, 2800 Victory Boulevard, Staten Island, NY 10314, USA.
[2] Present address: Corning SAS, 7bis avenue de Valvins, 77210 Avon, France.

1387-1811/$ - see front matter © 2006 Elsevier Inc. All rights reserved.
doi:10.1016/j.micromeso.2006.12.027

a catalyst to the carbon precursor or chemical vapor deposition of carbon can induce the formation of graphitic structures at much lower temperatures (818–1523 K) [2,5–8].

Some important beneficial features of graphitic carbons can be harnessed in materials with high surface area and readily accessible pores. However, except for the cases of graphitic carbon nanotubes (CNTs) [5,9–13] and certain other carbon nanostructures composed of curved, closed graphitic surfaces [14], creation of high surface area inherently involves an increase in the surface heterogeneity through the formation of edges and defects in the stacked graphene sheets. Another challenge is the formation of graphitic carbons with permanent porous structures, especially those with controlled pore size and shape.

In the early 1980s, Knox et al. [1] reported a silica-templated synthesis of graphitized porous carbon with a specific surface area of 150 $m^2 g^{-1}$ using a phenol–formaldehyde resin as a carbon precursor. Since then, this carbon has been commercially available as a packing material for high-performance liquid chromatography (HPLC). More recently, carbon suitable for application in monolithic HPLC columns was prepared using a polymer prepared from resorcinol/iron(III) complex and formaldehyde [2]. An appreciable degree of graphitization was achieved with iron catalyst at temperature as low as 1523 K. This graphitic material had a specific surface area of ~200 $m^2 g^{-1}$ with a contribution from micropores, and it had a rather low total pore volume. Li and Jaroniec [3] prepared a graphitized carbon from mesophase pitch, which was suitable for HPLC separations and had a specific surface area of 52 $m^2 g^{-1}$ and pore volume of 0.25 $cm^3 g^{-1}$. There are also numerous commercially available graphitized carbon blacks [15] with specific surface areas ranging from several to more than two hundred square meters per gram. Recently, there was some success in the synthesis of graphitized carbons with uniform pores of diameter in the mesopore range (2–50 nm) [16] or slightly above this size range. These carbons were prepared using the silica particles or silica colloidal crystals as templates. In particular, Li et al. synthesized mesoporous carbon from mesophase pitch using monodisperse silica particles to generate uniform pore voids with diameter of 24 nm, and graphitized this carbon under argon at ~2670 K [17]. The pore size decreased to 16 nm and the pore size distribution (PSD) broadened, but appreciable pore volume (0.72 $cm^3 g^{-1}$) and specific surface area (239 $m^2 g^{-1}$) were retained. Low-pressure nitrogen adsorption measurements suggested that the surface of this carbon was as homogeneous as that of Carbopack X (225 $m^2 g^{-1}$) graphitized carbon black [15], although PSD of the silica-particle-templated carbon was much narrower. More recently, an ordered macroporous carbon replica of colloidal-crystal silica was synthesized using a mesophase pitch as a precursor and was graphitized at 2773 K [18]. The resulting material was highly graphitic, as seen from X-ray diffraction (XRD), Raman spectroscopy and transmission electron microscopy (TEM). The pore diameter decreased from ~74 to ~65 nm, but the periodic pore structure was retained.

Recently, there has been a growing interest in the synthesis of ordered mesoporous carbons (OMCs) [19–21] with graphitic frameworks using ordered mesoporous silicas (OMSs) as templates [22–30]. First, Kim et al. [22] reported that OMCs synthesized from a polyaromatic hydrocarbon (acenaphthene) carbonized at 1173 K exhibited some degree of graphitic ordering in their frameworks. A wide-angle XRD pattern of one of these carbons featured quite narrow peaks (the (0 0 2) peak had a full width at half height of ~3°), and TEM images showed short graphene sheets stacked perpendicular to the surface of the material. Although the perfection of stacking was limited, the formation of semi-graphitic carbon structures as a result of the tendency of the carbon precursor to stack in a uniform way at low temperatures is quite remarkable. Stacking of imperfect graphene sheets perpendicular to the surface was also observed [28] for OMCs synthesized from mesophase pitch [28,31], whereas some extent of the alignment parallel to the surface was observed for OMCs synthesized from polypyrrole [29]. Fuertes and Centeno [25] synthesized OMC with a small content (~8 wt.%) of graphitic domains from pyrrole polymerized in the mesopores of OMS template impregnated with $FeCl_3$. The synthesis of OMCs with graphitic ordering in the framework was also pursued by Xia, Mokaya, and coworkers using CVD of acetonitrile at temperatures from 1123 to 1373 K [26,27,30]. Higher CVD temperatures allowed them to obtain graphitic carbons with mesoporous structures. The specific surface areas and pore volumes of these carbons were from 280 to 880 $m^2 g^{-1}$, and from 0.26 to 0.70 $cm^3 g^{-1}$, respectively, and they decreased as the CVD temperature was increased. In addition to these partially graphitic carbons synthesized without the high-temperature treatment, Fuertes and Alvarez [24] synthesized OMC from poly(vinyl chloride) (PVC) and heated it at ~2570 K for 0.5 h under argon atmosphere. The wide-angle XRD pattern for the resulting carbon featured (0 0 2) peak, which was very sharp, but appreciably broadened near the baseline. The graphitized carbon exhibited a single, very broad low-angle XRD peak, indicating some degree of local nanoscale ordering, although TEM showed a disordered structure. The obtained carbon exhibited a specific surface area of 260 $m^2 g^{-1}$, a pore volume of 0.34 $cm^3 g^{-1}$ and broad, perhaps bimodal, PSD.

Herein, it is shown that heat treatment at ~2470 K under argon atmosphere appreciably improves the atomic-scale ordering in frameworks of high-pore-volume mesoporous carbons [32] synthesized from polyacrylonitrile (PAN) using a templating method [32,33]. The evidence of the formation of graphitic structures was obtained from TEM, XRD and low-pressure nitrogen adsorption. The obtained partially graphitic carbons exhibited large mesopore volumes and high specific surface areas, although the carbons

templated by OMCs largely or completely lost their nanoscale ordering. These results suggest that it will be possible to successfully graphitize carbons derived from PAN using other synthesis approaches, such as a direct conversion of PAN-containing block copolymers [34–38] to nanostructured carbons [34,35,38].

2. Materials and methods

2.1. Materials

Ordered and disordered mesoporous carbons were synthesized using ordered mesoporous silicas (SBA-15 [39,40], FDU-1 [41,42]) and disordered silica gel Aldrich Si-150 as templates, and PAN as a carbon precursor, as described in detail elsewhere [32]. PAN was introduced to the pores of the templates through surface-initiated atom transfer radical polymerization (ATRP) [43–50]. The silica/PAN composites were converted to silica/carbon composites through the stabilization of PAN at 573 K under air, and carbonization at 1073 K under nitrogen. Subsequently, the silica templates were dissolved in an aqueous NaOH solution. The resulting carbon materials are denoted C-SBA-15, C-FDU-1 and C-Si-150, depending on the silica template used. As reported earlier [32], C-SBA-15 consisted of nanorods arranged in a two-dimensional hexagonal structure (and thus can be classified as OMC of the CMK-3 type [51]), C-FDU-1 was an array of ordered spheres (a similar material was also reported by Zhao et al. [52]), and C-Si-150 was a disordered carbon with a continuous structure. These carbons were heated under argon atmosphere (136 kPa) with a heating ramp of 10 K min^{-1} to ~2470 K, maintained at this temperature for 1 h, and cooled down to room temperature (the cooling took ~2 h). This treatment, which is herein referred to as "graphitization", was performed in a graphite furnace (Centorr/Vacuum Industries Inc., Model HP-2058). The resulting carbon samples are denoted as CG-SBA-15, CG-FDU-1 and CG-Si-150.

2.2. Characterization

Nitrogen adsorption isotherms were measured at 77 K using Micromeritics ASAP 2010 and ASAP 2020 gas adsorption analyzers. Before the adsorption measurements, samples were outgassed under vacuum at 473 K. TEM images were recorded using a JEOL JEM-2100 F TEM equipped with a CCD camera. Powder X-ray diffraction (XRD) patterns were recorded at wide angles on a Rigaku Geigerflex diffractometer using Cu Kα radiation. Small-angle X-ray scattering (SAXS) data were collected at CHESS D station at the synchrotron radiation source at Cornell University. The Raman spectra were collected on a Jobin Yvon T64000 triple Raman system (ISA, Edison, NJ) in subtractive mode with microprobe sampling optics. The excitation was at 514.5 nm (Ar^{+} laser, Model 95, Lexel Laser, Fremont, CA).

2.3. Calculations

The BET specific surface area [16] was calculated from nitrogen adsorption data in the relative pressure range from 0.04 to 0.2. The total pore volume [16] was estimated from the amount adsorbed at a relative pressure of ~0.99. The pore size distribution (PSD) was calculated using the algorithm outlined by Barrett, Joyner and Halenda (BJH) [53], and a relation between the capillary condensation pressure and the pore diameter established for cylindrical mesopores of silicas (the Kruk–Jaroniec–Sayari method) [54]. The relative adsorption was calculated by dividing the amount adsorbed by the BET monolayer capacity [15]. The size of graphitic domains, L, was estimated from XRD data using the Scherrer equation [55]: $L = k\lambda/(B\cos\theta)$, where λ is the wavelength of the X-rays, B is the peak width (full width at half height in radians), θ is the angle at which a given reflection is observed, and k is a constant. Following Knox et al. [1], $k = 0.84$ was used for evaluation of the stacking height of the graphitic domains from the width of the (002) reflection, whereas the k value of 1.84 was used for the evaluation of the lateral dimensions of the graphitic domains from the width of the asymmetric (100) peak (which may include (101) peak).

3. Results and discussion

3.1. Nitrogen adsorption, SAXS and TEM

As reported elsewhere [32], the templated mesoporous carbons from PAN exhibited nitrogen adsorption isotherms with prominent adsorption–desorption hysteresis loops and with capillary condensation steps located in the relative pressure interval from 0.6 to 0.95 (see Figs. 1–3). As can be seen in Figs. 1 and 2, the isotherms for the

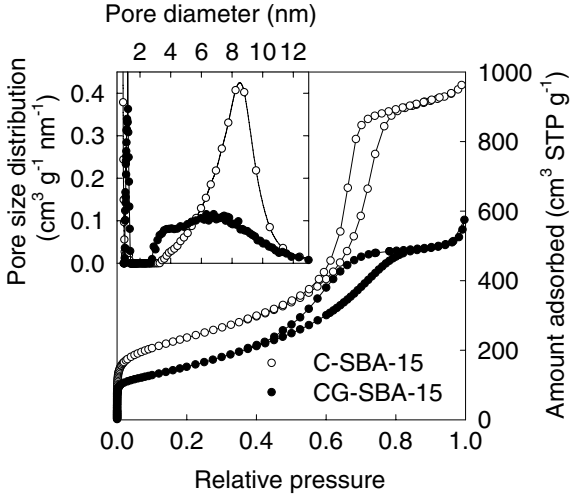

Fig. 1. Nitrogen adsorption isotherms and pore size distributions (inset) for carbon synthesized at 1073 K using ordered SBA-15 silica as a template, before (C-SBA-15) and after (CG-SBA-15) heating at ~2470 K under argon (data for C-SBA-15 are taken from Ref. [32]).

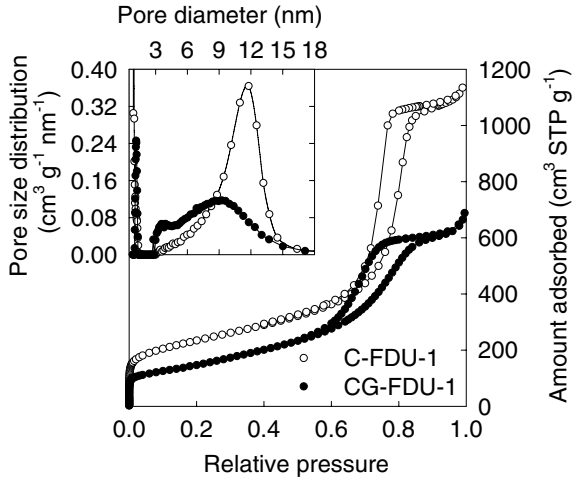

Fig. 2. Nitrogen adsorption isotherms and pore size distributions (inset) for carbon synthesized at 1073 K using ordered FDU-1 silica as a template, before (C-FDU-1) and after (CG-FDU-1) heating at ~2470 K under argon (data for C-FDU-1 are taken from Ref. [32]).

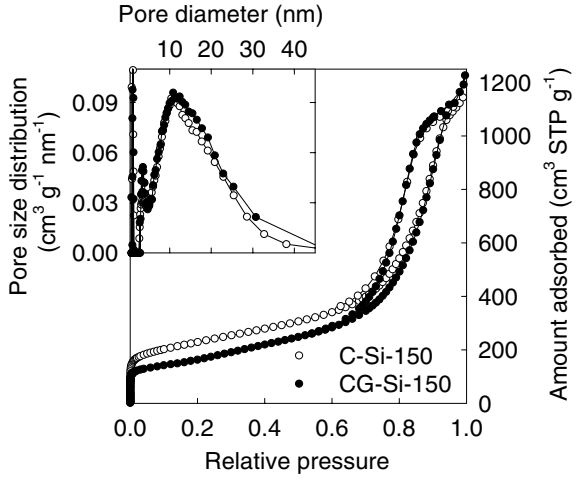

Fig. 3. Nitrogen adsorption isotherms and pore size distributions (inset) for carbon synthesized at 1073 K using disordered Si-150 silica as a template before (C-Si-150) and after (CG-Si-150) heating at ~2470 K under argon (data for C-Si-150 are taken from Ref. [32]).

OMCs heat-treated at 2470 K (CG-SBA-15 and CG-FDU-1) still featured pronounced capillary condensation steps, thus indicating the preservation of the mesoporosity during the graphitization. These isotherms leveled off after the completion of capillary condensation in the primary mesopores, which suggests that the high-temperature treatment did not lead to any appreciable development of large mesopore defects in the carbon frameworks. The heat treatment led to an appreciable decrease in the adsorption capacity, as already observed in the case of graphitization of carbons with large, spherical pores templated by silica colloidal particles or colloidal crystals [17,18]. In the case of C-SBA-15 carbon, the total pore volume decreased from 1.49 $cm^3\ g^{-1}$ to 0.85 $cm^3\ g^{-1}$, and the BET specific surface area decreased from 840 $m^2\ g^{-1}$ to 520 $m^2\ g^{-1}$ (~40% reduction). Also, the pore diameter decreased and PSD broadened (see Fig. 1). A similar PSD broadening and decrease in the total pore volume and specific surface area (from 1.75 to 1.03 $cm^3\ g^{-1}$ and from 830 to 520 $m^2\ g^{-1}$, respectively) was observed for C-FDU-1 (Fig. 2). Importantly, the overall decrease in adsorption capacity upon graphitization of our materials was much lower than that reported earlier [24] for a carbon replica of SBA-15 synthesized from PVC and graphitized at 2573 K for 30 min. In the latter case, the specific surface area was reduced from 930 to 260 $m^2\ g^{-1}$ and the mesopore volume decreased from 1.09 to 0.34 $cm^3\ g^{-1}$ (decrease by ~70%).

In contrast with the carbons templated by ordered mesoporous silicas, the C-Si-150 carbon templated by the disordered silica Si-150 fully retained its adsorption capacity after the same heat treatment at ~2470 K (see Fig. 3). PSD was also not altered to any appreciable extent (see Fig. 3, inset). Upon the heat treatment, the BET specific surface area decreased to ~70% of its original value (810 $m^2\ g^{-1}$ vs. 570 $m^2\ g^{-1}$), whereas the total pore volume remained essentially unchanged (1.77 $cm^3\ g^{-1}$ vs. 1.85 $cm^3\ g^{-1}$). This is a very important result, since to the best of our knowledge, the retention of the pore volume of a mesoporous carbon after a heat treatment at temperatures above 2270 K has not been reported. While this full retention of adsorption capacity might at first appear surprising, it should be pointed out that in principle, the graphitization of nanoporous carbon does not have to lead to a reduction in the pore volume per unit mass of the material. This is because the improvement of stacking order of graphene sheets does not have to lead to any significant shrinkage of the carbon framework, while the loss of oxygen-containing functional groups may reduce the mass of the carbonaceous structure without diminishing the void space in it. Thus, a typically observed prominent loss of pore volume upon graphitization may result from the susceptibility of carbon framework to local rearrangement and/or collapse.

The factors determining the extent of the mesopore volume change during the graphitization of our samples remain to be fully elucidated, but one can hypothesize that the connectivity between the parts of the carbon frameworks in materials subjected to graphitization determines the propensity for the pore volume loss. The inferred robustness of the C-Si-150 carbon synthesized using a disordered Si-150 silica template may result from its foam-like structure apparent in TEM images (see Supporting Figure S1). Moreover, the narrowness of the hysteresis loop on the adsorption isotherm of the Si-150 silica template [32] points to the lack of constrictions, whose presence would potentially weaken the framework of the templated carbon. On the other hand, the OMCs (C-SBA-15 and C-FDU-1) consisted of nanorods or nanospheres that were connected by bridges (otherwise the structure would not be sustainable), which were hardly visible (in the case of C-FDU-1) or not visible at all (in the case of C-SBA-15) by TEM. Consequently, there bridges were likely to be narrow and fragile,

and they apparently degraded or shrunk during the graphitization, leading to the loss of the ordered structure, with concomitant pore volume decrease. Regardless of the specific reasons for the pore volume decrease and loss of structural ordering upon graphitization for the OMCs from PAN, the results of the graphitization for their disordered counterpart suggest that it will be possible to convert an OMC from PAN into partially or fully graphitic structures without any appreciable loss of nanostructure ordering and mesopore volume. However, it will most likely require a selection of even more robust three-dimensional OMC frameworks.

The degree to which the nanoscale structure of the OMCs was retained upon graphitization was assessed with the aid of SAXS. The pattern for CG-SBA-15 was featureless (see Fig. 4), which indicates that the nanoscale ordering was lost. However, the pattern for the CG-FDU-1 sample still featured a pronounced shoulder, corresponding to the interplanar spacing of ~11 nm, thus providing evidence for a residual ordering in this sample. The observed interplanar spacing was ~20% lower than the interplanar spacing of 13.6 nm observed by SAXS (or XRD [32]) prior to the high-temperature treatment. It is clear that the graphitization led to the shrinkage of the structure (which is consistent with the pore diameter decrease, as discussed above) with concomitant decrease in the structural ordering. TEM imaging provided an indication of the retention of the particle morphology (see below), but little evidence of the retention of nanoscale ordering. A similar loss of the nanoscale ordering was also observed by others [24] upon graphitization of carbon replica of SBA-15 at ~2573 K, although in the latter case, the graphitized carbon, whose adsorption capacity was significantly reduced, still exhibited a very broad, low-angle peak on its XRD pattern.

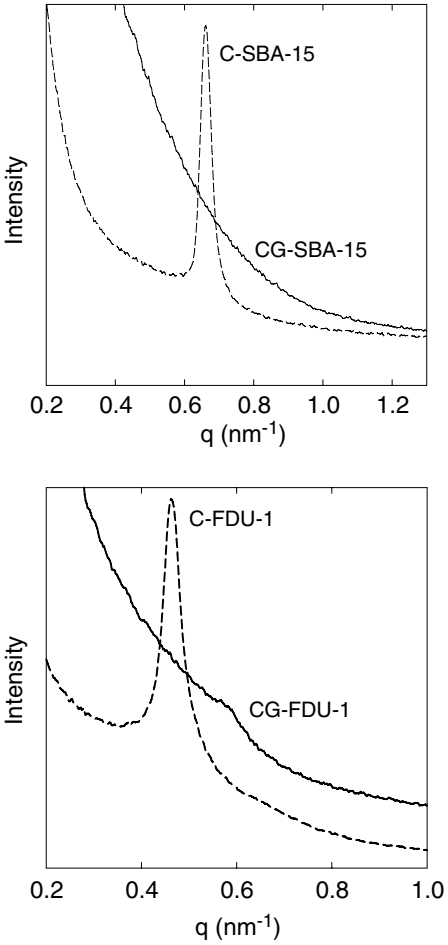

Fig. 4. Small-angle X-ray scattering patterns for carbons synthesized at 1073 K using ordered SBA-15 and FDU-1 silicas as templates, before (C-SBA-15 and C-FDU-1) and after (CG-SBA-15 and CG-FDU-1) heating at ~2470 K under argon.

3.2. XRD and high-resolution TEM

XRD patterns for the carbons are shown in Fig. 5. A typical diffraction pattern of non-graphitized carbon is represented by the data obtained for C-SBA-15 carbon, and featured characteristic broad (002) peak at ~24°, a less intense peak at ~44°, which corresponds to (101) and/or (100) reflections, and a hardly discernible feature at ~80°, which corresponds to the (110) reflection of a graphitic structure. The heat treatment decreased the width of the main (002) diffraction peak, and made the other two peaks (the (100) peak, perhaps with contribution from the (101) reflection [1], at ~43°, and the (110) peak at ~78°) more clearly visible. In addition, the main XRD peak for the graphitized samples appeared to be a superposition of a broader peak, and a narrow peak centered at

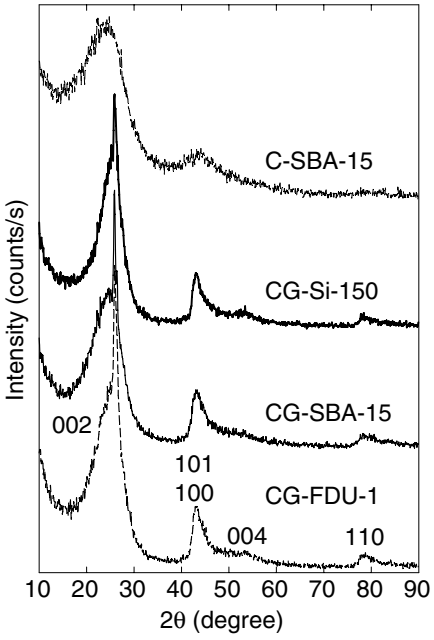

Fig. 5. XRD patterns (Cu Kα) acquired at wide angles for templated carbons carbonized at 1073 K, and heated at ~2470 K under argon (data for a non-graphitized C-SBA-15 sample, which are shown for comparison, are taken from Ref. [32]).

~25.9° (which corresponds to the interplanar spacing of 0.344 nm). This would suggest that minor parts of the samples are well graphitized, while major parts of the samples are graphitic to a smaller extent. On the basis of TEM images (see below), one can expect that the graphitization began primarily from the surface of the samples, but perhaps did not extend over the whole framework of the material. The increase in the high-temperature treatment time or temperature would probably result in more complete graphitization, but most likely at the expense of the specific surface area and pore volume. In principle, there is yet another possible explanation of the main XRD peak being a superposition of two peaks. Namely, the samples may contain highly graphitic domains that either originated from bulk non-templated carbon present in the samples, which can form during the carbonization by heating to 1073 K, as we have observed in some cases, or formed during the graphitization process, as observed by Knox et al. [1]. However, the presence of such bulk graphitic domains was not apparent from TEM images of our samples heat-treated at ~2470 K.

The size of graphitic domains was estimated using the Scherrer equation. For the graphitized samples CG-SBA-15 and CG-FDU-1, which were obtained from OMCs, the width of the broad component of the (002) peak was ~6° and thus the height of the stacks of graphene sheets was estimated as ~1.3 nm, which approximately corresponds to 4 graphene sheets. The width of the asymmetric (100) peak was ~3° and thus the lateral size of the graphene sheets can be estimated as ~6 nm. In the case of the graphitized carbon templated by disordered silica Aldrich Si-150, the peaks were somewhat narrower. The width of the (002) peak was ~5° and thus the height of the stacked graphene sheets was ~1.5 nm, which corresponds to 4–5 graphene sheets. It should be noted that if the calculations for any of these samples were performed on the basis of the width of the narrow spikes observed on the (002) peaks (see Fig. 5), the estimates of the average number of graphene sheets in single graphitic domains would be several times higher. The width of the (100) peak for the CG-Si-150 sample was ~2°, which allows one to estimate the lateral dimensions of the graphitic domains as ~9 nm.

Figs. 6–8 show TEM images of selected areas of CG-SBA-15, CG-FDU-1 and CG-Si-150 carbons. These images reveal the presence of numerous domains composed of series of parallel stripes with the spacing of ~0.34 nm (for CG-FDU-1 and CG-Si-150) or ~0.35 nm (for CG-SBA-15), as determined from Fourier transform analysis. There were somewhere between 2 and 20 stripes in each domain, whereas the length of straight segments of the domains was typically 5–20 nm, although the length of continuous, twisted graphene sheets was in some cases larger. It is noteworthy that the results of calculations of sizes of graphitic domains from the Scherrer equation compare fairly well with the features observed by TEM. The images provided some indication that the graphitization proceeded from the surface of the material inwards, since the edges of the particles seemed to be typically composed of graphitic domains parallel to the surface (edge of particle), similar to the results reported in [29]. The lower-magnification image of the CG-SBA-15 (Supporting Figure S2) showed features similar to those observed on TEM images for the nongraphitized SBA-15-templated carbons (see Supporting Figure S3), which suggests the preservation of the particle morphology during the heat treatment at 2470 K. However, there was no appreciable evidence of the preservation of the nanoscale ordering, which was present in C-SBA-15

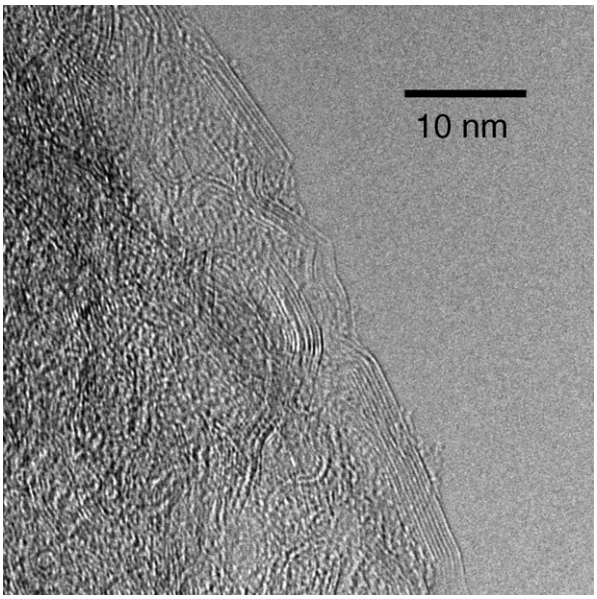

Fig. 6. TEM image for high-temperature-treated carbon CG-SBA-15 synthesized using ordered SBA-15 silica as a template.

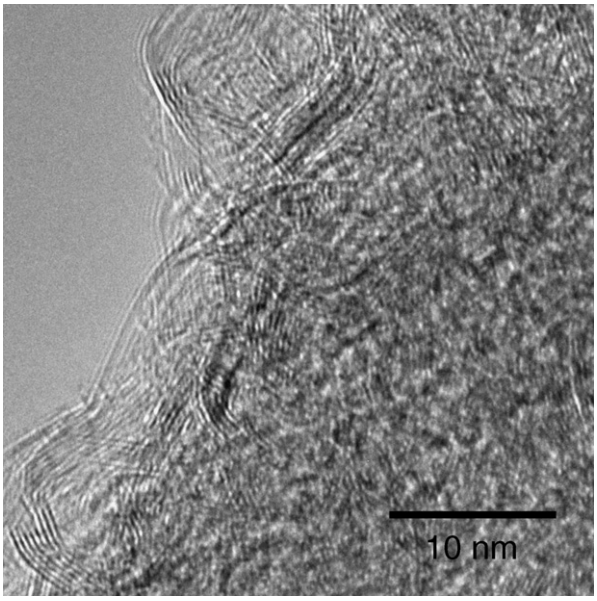

Fig. 7. TEM image for high-temperature-treated carbon CG-FDU-1 synthesized using ordered FDU-1 silica as a template.

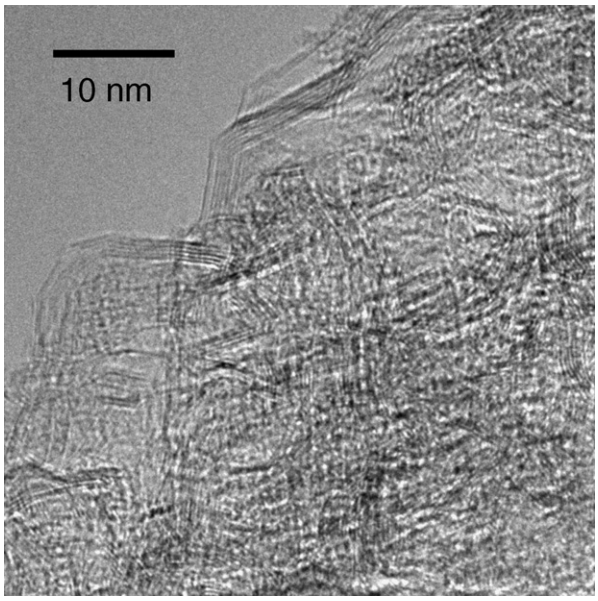

Fig. 8. TEM image for high-temperature-treated carbon CG-Si-150 synthesized using disordered Si-150 silica as a template.

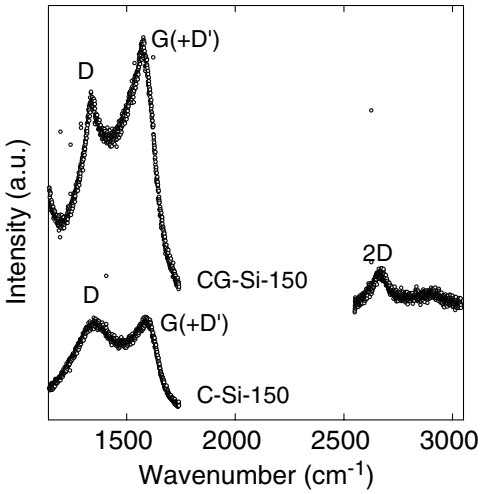

Fig. 9. Raman spectra for Si-150-templated carbon, before (C-Si-150) and after (CG-Si-150) heating at ~2470 K under argon.

and C-FDU-1 samples prior to the high-temperature treatment. This TEM observation is consistent with the low-angle XRD data. Supporting Figures S4 and S5 show larger areas of the high-temperature-treated materials imaged at lower magnifications. Quite uniformly distributed dark, striped features can be identified as graphitic domains. These images provided the evidence that the graphitic domains were uniformly distributed in the structure of the materials, rather than being formed primarily on the edges of the particles.

3.3. Raman spectroscopy

Raman spectra for one of the carbons before and after the heat treatment at ~2470 K are shown in Fig. 9. The spectra featured two major peaks centered at ~1340 cm^{-1} and ~1580 cm^{-1}. For sp^2 carbon materials, the peak at about 1340 cm^{-1} is usually referred to as the D band, whereas the peak at about 1580 cm^{-1} is referred to as the G band, although the latter is likely to be a combination of the G and the D′ bands [56]. The G band arises from the vibrational mode of ideal graphene sheets [56]. The D and D′ bands, which are typically observed at ~1350 cm^{-1} and ~1620 cm^{-1}, arise from vibrations of disordered graphene sheets, with disorder being introduced by the presence of edges and/or heteroatoms (such as nitrogen). To this end, although the content of nitrogen was not determined in the carbons considered herein, but it is likely to be negligibly small, because earlier studies suggest that during carbonization of PAN, the elimination of heteroatoms is essentially complete below 1873 K [57,58]. For the heat-treated samples, the G band (perhaps with a contribution from the D′ band) at ~1580 cm^{-1} was typically much more prominent than the D band at ~1340 cm^{-1}, unlike in the case of the carbon before the heat treatment, for which the D band and G (+D′) band were of similar intensity. However, in both cases, these bands were quite broad and they were not well separated. The observed changes in the Raman spectra indicate an increase in the content of uniform graphitic structures as a result of the heat treatment at ~2470 K. For the sample heat-treated at ~2470 K, there was also a clearly pronounced 2D band [56,59] at around 2650 cm^{-1}, which is another indication of a higher extent of graphitic ordering [56]. Some other less well-defined Raman spectra were also collected in other areas of the samples, suggesting a certain degree of inhomogeneity in the carbons graphitized under conditions discussed here.

3.4. Low-pressure nitrogen adsorption

Low-pressure nitrogen adsorption was used to investigate the surface properties of the carbons from PAN after the heat treatment at ~2470 K. It is known that low-pressure nitrogen adsorption at 77 K on carbon surfaces with a sufficient degree of homogeneity (the surfaces of graphitized carbons) proceeds via the formation of a monolayer of nitrogen molecules, followed by the formation of subsequent layers (multilayer adsorption). The formation of a monolayer of N_2 molecules in a narrow relative pressure range suggests that the surface has adsorption sites that exhibit similar energies of interactions with nitrogen molecules. Ideal graphitic basal planes are highly homogeneous surfaces [60–62], but they may feature defects, and typically have edges decorated with covalently bonded hydrogen atoms, oxygen-containing groups and so forth. The presence of defects and edges makes the surface less homogeneous with respect to adsorbed molecules [62]. Consequently, adsorption properties, and low-pressure adsorption properties in particular, are related to the

degree of perfection of carbon surfaces, which for the materials considered here is related to the degree of graphitization [15].

To facilitate the comparison of low-pressure adsorption data for different samples, each isotherm was expressed as a reduced adsorption curve, which provides the amount adsorbed divided by the BET monolayer capacity [15]. It should be noted that the reduced adsorption equal to 1.0 corresponds to the attainment of a statistical monolayer on the surface (within the accuracy of the BET specific surface area calculations). The surface properties of samples are primarily reflected in the submonolayer adsorption data [62]. As shown in Fig. 10, the reduced adsorption curves featured steps centered at relative pressures of 10^{-4}–10^{-3}, which can be attributed to the formation of a monolayer of nitrogen molecules on the surface of the carbons. The reduced adsorption isotherms for our high-temperature-treated carbon samples were similar to that of the high-surface-area graphitized carbon black Carbopack X (specific surface area of 225 $m^2 g^{-1}$) [15], suggesting that the surface properties of these carbons are similar. This is a very good result, taking into consideration that our high-temperature-treated carbons have specific surface areas about 2.5 times higher than that of Carbopack X, and it is known from an earlier study [15] that the surface of graphitized porous carbons tends to be more heterogeneous for samples with higher specific surface areas. For instance, the most homogeneous surface (as seen from gas adsorption data that are also included in Fig. 10) was observed for Carbopack F with a specific surface area of 6.2 $m^2 g^{-1}$. Consequently, on the basis of their specific surface areas of 500–600 $m^2 g^{-1}$, our graphitized carbons would be expected to have much less homogeneous surfaces than the surface of Carbopack X (225 $m^2 g^{-1}$), whereas in fact, these surfaces appeared to be similarly homogeneous. It is clear that the surfaces of the present samples are not as homogeneous as the surface of the highly graphitized carbon black Carbopack F, perhaps as a result of a limited size of graphitic domains and the resultant edge effects, or lower degree of perfection of ordering within the graphitic layers. Perhaps also a certain part of the surface exposed to nitrogen gas was weakly graphitized. Anyway, our graphitized samples had surfaces that were clearly much more homogeneous than the surface of a typical non-graphitized carbon black Cabot BP 280 [15,63]. It should be noted that earlier studies of Darmstadt et al. [64] showed that the heat treatment at ~1870 K appreciably decreased the surface heterogeneity (which suggests increased atomic scale ordering) for OMCs from sucrose. However, the comparison of low-pressure adsorption data reported by Darmstadt et al. [64] with the data for our samples suggests that the latter have more homogeneous surfaces.

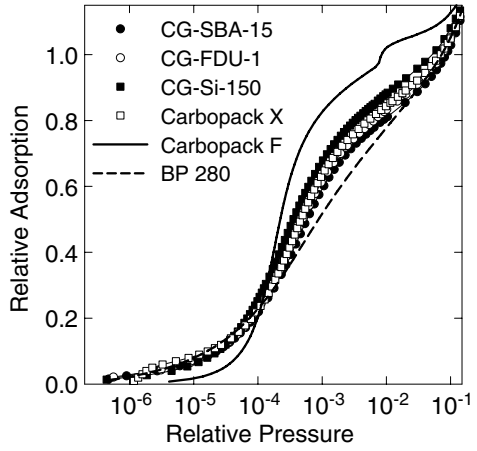

Fig. 10. Low-pressure parts of nitrogen adsorption isotherms for the carbons heated at ~2470 K under argon, shown as relative adsorption curves. The data for commercially available graphitized carbon blacks Carbopack X and F, and for a non-graphitized carbon black Cabot BP 280 (taken from Ref. [15]) are shown for comparison.

The low uptake of nitrogen at relative pressures below 10^{-5} for the PAN-derived carbons heat-treated at ~2470 K suggests the absence of any detectable microporosity. In contrast, our carbons prior to the high-temperature treatment exhibited micropore volumes of 0.06–0.10 $cm^3 g^{-1}$ (~5% of their total pore volume) [32], which are appreciable (although they are low in comparison to the micropore volumes of most of other mesoporous carbons reported in the literature). For mesoporous–microporous materials, the low-pressure adsorption is a combination of: (i) the monolayer–multilayer adsorption on the mesopore surface, and (ii) the micropore filling (for narrower micropores) and enhanced adsorption on the micropore surface (for wider micropores). Consequently, the data that provide information about the surface properties of such materials cannot be readily separated from the data that reflect both the surface properties and the micropore size distribution. Therefore, the comparison of surface properties of PAN-derived carbons before and after graphitization was not attempted.

4. Conclusions

The described results demonstrate the synthesis of partially graphitic high-surface-area carbons with very high mesopore volumes, using PAN as a precursor and mesoporous silicas as templates. The heat treatment of mesoporous carbons from PAN at ~2470 K under argon induced the formation of graphitic domains, significantly enhanced the surface homogeneity and eliminated the microporosity. This was paralleled by a moderate reduction of the specific surface area (by 30–40%), whereas the pore volume was either reduced (by up to 40%) or remained essentially unchanged. The domains with an appreciable degree of perfection in the stacking of graphene sheets were observed by TEM in carbons derived from OMCs, which appears to be the first direct observation of such structures in products of high-temperature treatment of OMCs. The nanoscale ordering of OMCs was largely or completely lost after

the high-temperature treatment, but the thermal stability of the disordered carbon suggests that it will be possible to graphitize PAN-derived OMCs of appropriate structures with retention of their nanoscale ordering.

Acknowledgments

The support from NSF Grant DMR-0304508 is gratefully acknowledged. K.M. also acknowledges support from NSF Grant DMR-0090409. Abigail M. Laurent and Dr. Todd Przybycien (Carnegie Mellon University) are acknowledged for help in the Raman spectroscopy measurements. SAXS measurements conducted at the Cornell High Energy Synchrotron Source (CHESS), which is supported by the National Science Foundation under award DMR-0225180. Dr. Detlef-M. Smilgies (CHESS, Cornell University) is gratefully acknowledged for assistance in the SAXS measurements. Noel T. Nuhfer is acknowledged for assistance in TEM analysis for non-graphitized carbons.

Appendix A. Supplementary data

Five (5) TEM images for graphitized and non-graphitized carbons. Supplementary data associated with this article can be found, in the online version, at doi:10.1016/j.micromeso.2006.12.027.

References

[1] J.H. Knox, B. Kaur, G.R. Millward, J. Chromatogr. 352 (1986) 3.
[2] C. Liang, S. Dai, G. Guiochon, Anal. Chem. 75 (2003) 4904.
[3] Z. Li, M. Jaroniec, Anal. Chem. 76 (2004) 5479.
[4] J.-B. Donnet, T.K. Wang, S. Rebouillat, J.C.M. Peng (Eds.), Carbon fibers, Marcel Dekker Inc., New York, 1998.
[5] G. Che, B.B. Lakshmi, C.R. Martin, E.R. Fisher, R.S. Ruoff, Chem. Mater. 10 (1998) 260.
[6] S. Han, Y. Yun, K.-w. Park, Y.-e. Sung, T. Hyeon, Adv. Mater. 15 (2003) 1922.
[7] M. Sevilla, A.B. Fuertes, Carbon 44 (2006) 468.
[8] A.-H. Lu, W.-C. Li, E.-L. Salabas, B. Spliethoff, F. Schueth, Chem. Mater. 18 (2006) 2086.
[9] S. Iijima, Nature 354 (1991) 56.
[10] A. Thess, R. Lee, P. Nikolaev, H. Dai, P. Petit, J. Robert, C. Xu, Y.H. Lee, S.G. Kim, et al., Science 273 (1996) 483.
[11] T. Kyotani, L.-f. Tsai, A. Tomita, Chem. Mater. 8 (1996) 2109.
[12] J.M. Nhut, L. Pesant, J.P. Tessonnier, G. Wine, J. Guille, C. Pham-Huu, M.J. Ledoux, Appl. Catal. A 254 (2003) 345.
[13] J. Jang, J.H. Oh, Chem. Commun. (2004) 882.
[14] S. Bandow, F. Kokai, K. Takahashi, M. Yudasaka, L.C. Qin, S. Iijima, Chem. Phys. Lett. 321 (2000) 514.
[15] M. Kruk, Z. Li, M. Jaroniec, W.R. Betz, Langmuir 15 (1999) 1435.
[16] K.S.W. Sing, D.H. Everett, R.A.W. Haul, L. Moscou, R.A. Pierotti, J. Rouquerol, T. Siemieniewska, Pure Appl. Chem. 57 (1985) 603.
[17] Z. Li, M. Jaroniec, Y.-J. Lee, L.R. Radovic, Chem. Commun. (2002) 1346.
[18] S.B. Yoon, G.S. Chai, S.K. Kang, J.-S. Yu, K.P. Gierszal, M. Jaroniec, J. Am. Chem. Soc. 127 (2005) 4188.
[19] R. Ryoo, S.H. Joo, S. Jun, J. Phys. Chem. B 103 (1999) 7743.
[20] J. Lee, S. Yoon, T. Hyeon, S.M. Oh, K.B. Kim, Chem. Commun. (1999) 2177.
[21] S. Tanaka, N. Nishiyama, Y. Egashira, K. Ueyama, Chem. Commun. (2005) 2125.
[22] T.-W. Kim, I.-S. Park, R. Ryoo, Angew. Chem. Int. Ed. 42 (2003) 4375.
[23] C.H. Kim, D.-K. Lee, T.J. Pinnavaia, Langmuir 20 (2004) 5157.
[24] A.B. Fuertes, S. Alvarez, Carbon 42 (2004) 3049.
[25] A.B. Fuertes, T.A. Centeno, J. Mater. Chem. 15 (2005) 1079.
[26] Y. Xia, Z. Yang, R. Mokaya, J. Phys. Chem. B 108 (2004) 19293.
[27] Y. Xia, R. Mokaya, Adv. Mater. 16 (2004) 1553.
[28] H. Yang, Y. Yan, Y. Liu, F. Zhang, R. Zhang, Y. Meng, M. Li, S. Xie, B. Tu, D. Zhao, J. Phys. Chem. B 108 (2004) 17320.
[29] C.-M. Yang, C. Weidenthaler, B. Spliethoff, M. Mayanna, F. Schueth, Chem. Mater. 17 (2005) 355.
[30] Y. Xia, R. Mokaya, Chem. Mater. 17 (2005) 1553.
[31] Z. Li, M. Jaroniec, J. Phys. Chem. B 108 (2004) 824.
[32] M. Kruk, B. Dufour, E.B. Celer, T. Kowalewski, M. Jaroniec, K. Matyjaszewski, J. Phys. Chem. B 109 (2005) 9216.
[33] A. Lu, A. Kiefer, W. Schmidt, F. Schueth, Chem. Mater. 16 (2004) 100.
[34] T. Kowalewski, N.V. Tsarevsky, K. Matyjaszewski, J. Am. Chem. Soc. 124 (2002) 10632.
[35] C.B. Tang, A. Tracz, M. Kruk, R. Zhang, D.M. Smilgies, K. Matyjaszewski, T. Kowalewski, J. Am. Chem. Soc. 127 (2005) 6918.
[36] C. Tang, T. Kowalewski, K. Matyjaszewski, Macromolecules 36 (2003) 8587.
[37] C. Tang, T. Kowalewski, K. Matyjaszewski, Macromolecules 36 (2003) 1465.
[38] C. Tang, K. Qi, K.L. Wooley, K. Matyjaszewski, T. Kowalewski, Angew. Chem. Int. Ed. 43 (2004) 2783.
[39] D. Zhao, J. Feng, Q. Huo, N. Melosh, G.H. Frederickson, B.F. Chmelka, G.D. Stucky, Science 279 (1998) 548.
[40] R. Ryoo, C.H. Ko, M. Kruk, V. Antochshuk, M. Jaroniec, J. Phys. Chem. B 104 (2000) 11465.
[41] C. Yu, Y. Yu, D. Zhao, Chem. Commun. (2000) 575.
[42] J.R. Matos, M. Kruk, L.P. Mercuri, M. Jaroniec, L. Zhao, T. Kamiyama, O. Terasaki, T.J. Pinnavaia, Y. Liu, J. Am. Chem. Soc. 125 (2003) 821.
[43] K. Matyjaszewski, J. Xia, Chem. Rev. 101 (2001) 2921.
[44] K. Matyjaszewski, S.M. Jo, H.-j. Paik, S.G. Gaynor, Macromolecules 30 (1997) 6398.
[45] K. Matyjaszewski, S.M. Jo, H.-j. Paik, D.A. Shipp, Macromolecules 32 (1999) 6431.
[46] K. Matyjaszewski, P.J. Miller, N. Shukla, B. Immaraporn, A. Gelman, B.B. Luokala, T.M. Siclovan, G. Kickelbick, T. Vallant, H. Hoffmann, T. Pakula, Macromolecules 32 (1999) 8716.
[47] J. Pyun, K. Matyjaszewski, Chem. Mater. 13 (2001) 3436.
[48] K.A. Davis, K. Matyjaszewski, Adv. Polym. Sci. 159 (2002) 1.
[49] J. Pyun, T. Kowalewski, K. Matyjaszewski, Macromol. Rapid Commun. 24 (2003) 1043.
[50] J. Pyun, K. Matyjaszewski, T. Kowalewski, D. Savin, G. Patterson, G. Kickelbick, N. Huesing, J. Am. Chem. Soc. 123 (2001) 9445.
[51] S. Jun, S.H. Joo, R. Ryoo, M. Kruk, M. Jaroniec, Z. Liu, T. Ohsuna, O. Terasaki, J. Am. Chem. Soc. 122 (2000) 10712.
[52] J. Fan, C. Yu, F. Gao, J. Lei, B. Tian, L. Wang, Q. Luo, B. Tu, W. Zhou, D. Zhao, Angew. Chem. Int. Ed. 42 (2003) 3146.
[53] E.P. Barrett, L.G. Joyner, P.P. Halenda, J. Am. Chem. Soc. 73 (1951) 373.
[54] M. Kruk, M. Jaroniec, A. Sayari, Langmuir 13 (1997) 6267.
[55] P. Scherrer, Nachr. Ges. Wiss. Gottingen (1918) 96.
[56] A. Sadezky, H. Muckenhuber, H. Grothe, R. Niessner, U. Poschl, Carbon 43 (2005) 1731.
[57] T. Kyotani, N. Sonobe, A. Tomita, Nature 331 (1988) 331.
[58] N. Sonobe, T. Kyotani, Y. Hishiyama, M. Shiraishi, A. Tomita, J. Phys. Chem. 92 (1988) 7029.
[59] Y. Wang, D.C. Alsmeyer, R.L. McCreery, Chem. Mater. 2 (1990) 557.

[60] J.K. Kjems, L. Passell, H. Taub, J.G. Dash, A.D. Novaco, Phys. Rev. B 13 (1976) 1446.
[61] T.T. Chung, J.G. Dash, Surf. Sci. 66 (1977) 559.
[62] M. Jaroniec, R. Madey, Physical Adsorption on Heterogeneous Solids, Elsevier, Amsterdam, 1988.
[63] M. Kruk, M. Jaroniec, K.P. Gadkaree, J. Colloid Interface Sci. 192 (1997) 250.
[64] H. Darmstadt, C. Roy, S. Kaliaguine, S.H. Joo, R. Ryoo, Microporous Mesoporous Mater. 60 (2003) 139.